International Journal Of Core Engineering & Management (ISSN: 2348-9510)
Special Issue, NCIAEE-2017, St. Johns College of Engineering and Technology, Yemmiganur

A NON-LINEAR MODEL PREDICTIVE CONTROL (NMPC) ENERGY MANAGEMENT CONTROL STRATEGY FOR STANDALONE DC MICROGRIDS

A.Santhosh Kumar[1], E.Ramakrishna[2], S.Shamshul Haq[3]

[1]PG student, Department of Electrical and Electronics Engineering, SJCET, Yemmiganur, Kurnool [D],A.P
[2]Associate Professor & HOD, Department of Electrical and Electronics Engineering, SJCET, Yemmiganur, Kurnool [D],A.P
[3] Associate professor, Department of Electrical and Electronics Engineering, SJCET, Yemmiganur, Kurnool [D],A.P

Abstract

This paper comprises of developing an Energy Management Strategy that dynamically optimizes the operation of stand-alone dc microgrids, consisting of wind, photovoltaic (PV) and battery branches, and coordinately manage all energy flows in order to achieve four control objectives i.e regulating dc bus voltage level of microgrids; proportional power sharing between generators as a local droop control realization; charging batteries as close to IU regime as possible; and tracking MPPs of wind and PV branches during their normal operations. Non-linear model predictive control (NMPC) strategies are inherently multivariable and handle constraints and delays. In this paper, the above mentioned EMS is developed as an NMPC strategy to extract the optimal control signals, which are duty cycles of three DC-DC converters and pitch angle of a wind turbine. The variable load demands are also shared accurately between generators in proportion to their ratings. Moreover, the DC bus voltage is regulated within a predefined range, as a design parameter.

Keywords: Battery Management, generation curtailment, maximum power point tracking (MPPT), nonlinear model predictive control (NMPC), power sharing, renewable energy, voltage regulation.

I. INTRODUCTION

The classical energy management strategies employ the maximum power point tracking (MPPT) algorithms and rely on batteries in case of possible excess or deficit of energy. However, in order to realize constant current-constant voltage (IU) charging regime and increase the life span of batteries, energy management strategies require being more flexible with the power curtailment feature. In this paper, a coordinated and multivariable energy management strategy is proposed that employs a wind turbine and a photovoltaic array of a standalone DC microgrid as controllable generators by adjusting the pitch angle and the switching duty cycles.

The near future distribution networks will consist of several interconnected microgrids that will locally generate, consume, and store energy [1]. A microgrid may operate as an extension of the main grid, i.e., grid-connected, or as a standalone network with no connection to the grid. Standalone dc microgrids have some distinct applications in avionic, automotive, or marine industries, as well as remote rural areas. While ac systems suffer from the need of synchronization of several generators [2],

[3], dc microgrids are more efficient due to the fact that dc generators and storages do not need ac-dc converters for being connected to dc microgrids [4], [1]. The three well-known issues regarding voltage regulation, power sharing, and battery management, are more severe in standalone green microgrids that consist of only intermittent solar and wind energy sources, and lead to the necessity of more sophisticated control strategies. The stability of a dc microgrid is measured in terms of the stability of its dc bus voltage level [5], [6], which is one of the main control objectives [7].

The grid voltage source converters (G-VSCs) are the primary slack terminals to regulate the voltage level of grid-connected microgrids (e.g., [5], [6], [8], [9]). Battery banks, on the other hand, are effective slack terminals for standalone microgrids [6]; however, their energy absorbing capacities are limited regarding a number of operational constraints, as explained later in this section. In order to regulate the voltage level of standalone dc microgrids, the works in [2] and [6] present load shedding strategies for the cases in which there is insufficient power generation or energy storage. The works in [10]–[12], on the other hand, present strategies that curtail the renewable power generations of standalone dc microgrids if the battery bank cannot absorb the excess generation.

In order to prevent over-stressing conditions and circulating currents between generators [13], load demands need to be shared between all slack DGs in proportion to their ratings [7], [14]. The works in [3], [7], [13], and [15]–[18] extend the conventional droop control technique [11] for dc slack terminals by replacing the conventional curves with either dc power-dc voltage or a dc voltage-output current curve However, standalone dc microgrids are usually located in small-scale areas where the power sharing between DGs can be managed by centralized algorithms which are less affected by two issues: 1) batteries in charging mode are nonlinear loads causing distortions to the grid voltage; and 2) the absolute voltage level of a standalone microgrid is shifted as the result of the load demand variation. A number of phenomena affect the batteries operation during the charging mode [19]:
1)applying high charging currents, the batteries voltages quickly reach to the gassing threshold; 2) the internal resistor and hence power losses and thermal effects increase at high SOC levels; and 3) batteries cannot be fully charged with a constant high charging current. The work in [6] limits, as an operational constraint, the maximum absorbed power by the batteries in order to protect them from being over-charged. However, since batteries act as nonlinear loads during the charging mode, it does not necessarily limit the charging currents. Alternatively, the works in [10] restricts the maximum attainable SOC that leads to unused capacities.

Depending on the proportion of the power generation to the load demand ratio within standalone DC microgrids, three cases are envisaged: 1) power generation and load demand are balanced; 2) load demand exceeds power generation causes dc bus voltage to drop in absence of any load shedding; and 3) power generation is higher than load demand leads batteries to be over-charged and bus voltage to climb. This study focuses on case 3) in which the generated power must be curtailed if it violates the batteries charging rates or if batteries are fully charged. A novel energy management strategy (EMS) is proposed to ad-dress, as its control objectives, three aforementioned issues corresponding standalone dc microgrids; i.e., dc bus voltage regulation, proportional power sharing, and battery management. In contrast to the strategies available in literature in which renewable energy systems (RESs) always operate in their MPPT mode, the proposed multivariable strategy uses a wind turbine and a PV array as controllable generators and curtails their generations if it is necessary. The proposed EMS is developed as an online novel NMPC strategy that continuously solves an optimal control problem (OCP) and finds the optimum values of the pitch angle and three switching duty cycles. It simultaneously controls four variables of microgrids: 1) power coefficient of

the wind turbine; 2) angular velocity of the wind generator; 3) operating voltage of the PV array; and 4) charging current of the battery bank. It is shown that, employing new available non-linear optimization techniques and tools, the computational time to solve the resulting NMPC strategy is in permissible range. Unlike dump load-based strategies that only protect the battery from over charging, the proposed strategy implements the IU charging regime that helps to increase the batteries life span. Moreover, removing dump loads, the overall installation cost is reduced.

This paper is organized as follows: Section II presents the mathematical model of standalone dc microgrids. Section III shows the presented EMS as an OCP problem which is realized as a NMPC-based strategy. Section IV presents and discusses the obtained results. Finally, the conclusion of the study is given in Section V.

II. SYSTEM DESCRIPTIONS AND MODELLING

The standalone dc microgrid in Fig. 1 is a small-scale micro-grid for remote applications. The wind turbine operates at variable speeds and is connected to the electrical generator directly, i.e., the direct-drive coupling. The variable speed operation is more flexible for the power management and MPPT applications [21]. Furthermore, direct-drive coupling is more efficient and reliable and is more popular for small-scale wind turbines. In spite of high cost, permanent magnet synchronous generators (PMSGs) are the most dominant type of direct-drive generators in the market [22], chiefly due to higher efficiency.

From Fig. 1, it can be seen that battery bank is connected to the dc bus through a dc-coupled structure, i.e., via a dc-dc converter, which is more flexible in terms of implementing different charging and discharging regimes despite more power losses [19].

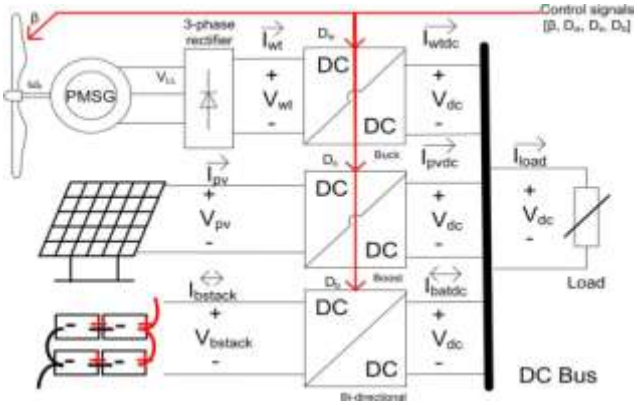

Fig 1: Topology of a small-scale and standalone dc microgrid

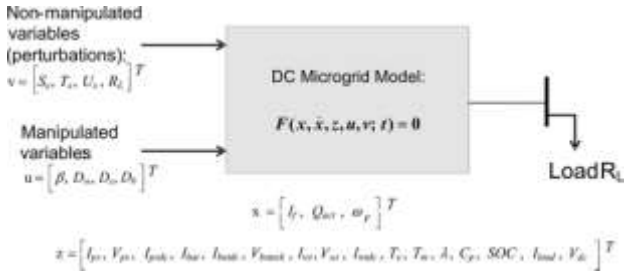

Fig 2: Modified version of the system model

Fig. 2 summarizes a modified version of the proposed model in [20]. Since this paper focuses on the case in which there is an excess power greater than or equal to the maximum possible absorbing rate of the battery bank, the hybrid nature of the battery bank operation is ignored for the sake of simplicity. The differential and algebraic states, i.e., x and z, and the manipulated and non-manipulated control variables, namely, u and v, are detailed later throughout the next sub-sections.

where $\mathfrak{J}$ is a set of implicit differential and algebraic functional f_i for $i \in \{1, 2, .., 24\}$.
The first two constraints f_1 and f_2 are due to the fact that in standalone dc microgrids the sum of the generated, stored and consumed powers is always zero:

$$f_1 = V_{dc}\left(I_{pvdc} + I_{wtdc} + I_{batdc} - I_{load}\right), \quad (2a)$$
$$f_2 = V_{dc} - I_{load}R_L. \quad (2b)$$

A. Wind Branch

Performance of the wind turbines is measured as the power coefficient curve with respect to the tip speed ratio and pitch angle [23]. Equation (3) shows the power coefficient curve of three-blade wind turbines [24]:

$$f_3 = C_{p,norm} - \frac{1}{C_{p,\max}} \times (C_1(\frac{C_2}{\lambda_i} - C_3\beta - C_4)\exp(-\frac{C_5}{\lambda_i}) + C_6\lambda),$$
$$f_4 = \lambda - \frac{Rad \times \omega_r}{U_z},$$
$$f_5 = \lambda_i - (\frac{1}{\lambda + 0.08\beta} - \frac{0.035}{\beta^3 + 1})^{-1},$$

B. Battery Branch

$$\mathcal{F}(\mathrm{x}, \dot{\mathrm{x}}, \mathrm{z}, \mathrm{u}, \mathrm{v}) = \begin{bmatrix} f_1(\mathrm{x}, \dot{\mathrm{x}}, \mathrm{z}, \mathrm{u}, \mathrm{v}) \\ f_2(\mathrm{x}, \dot{\mathrm{x}}, \mathrm{z}, \mathrm{u}, \mathrm{v}) \\ f_{24}(\mathrm{x}, \dot{\mathrm{x}}, \mathrm{z}, \mathrm{u}, \mathrm{v}) \end{bmatrix} = 0 \quad (1)$$

The charging operation of a lead acid battery bank, consisting of N_{batp} x N_{bats} batteries, is modelled as (8) [26].where V_{bstack}, I_{bstack}, and SOC are respectively the voltage, current and state of charge of the battery bank. I_f is the filtered value of the battery current with the time constant of T_s and Q_{act} is the actual battery capacity. The experimental parameter P_1 requires being identified for each type of battery while the maximum amount of the battery capacity, C_{max}, internal resistor of the battery, R_{bat} and the battery constant voltage, V_o are given by manufacturers.

By ignoring the discharging mode of the battery bank operation, the bi-directonal converter acts as a boost-type converter [(8d)-(8e)].

C. Solar Branch

The equivalent electrical circuit of the PV module [27], [28] is used to mathematically model the solar branch, consisting of a PV array and a boost converter [29].

D. Control System

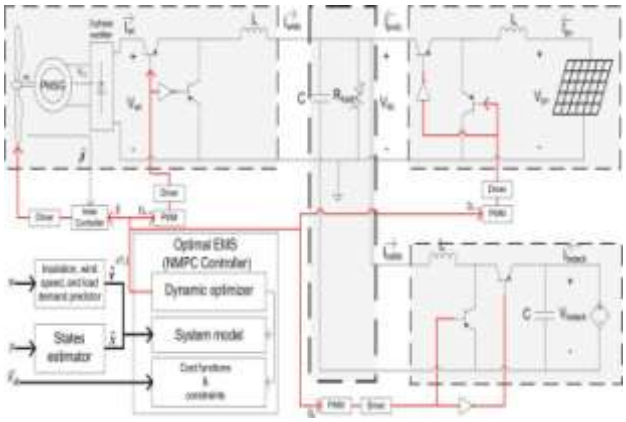

Fig 3: Simplified view of the dc microgrid and the developed NMPC controller. The battery bank is assumed to work in charging mode

III. OVERVIEW

Thanks to the multilevel energy storage, the intermittent and volatile renewable power outputs can be managed, and a deterministic controlled power to the main grid is obtained by optimization. Providing uninterruptible power supply (UPS) service to loads when needed is a core duty of the urban microgrid. EV fast charging introduces a stochastic load to the microgrid. The multilevel energy storage mitigates potential impacts on the main grid. In building integration, a vertical axis wind turbine may be installed on the rooftop as shown in Fig. 5.2. PV panels can be co-located on the rooftop and the facade of the building. Such or similar configurations benefit from a local availability of abundant wind and solar energy. The fast charging station is realized for public access at the ground level. It is connected close to the LV–MV transformer to reduce losses and voltage drop. EVs parked in the building are offered smart charging within user-defined constraints.

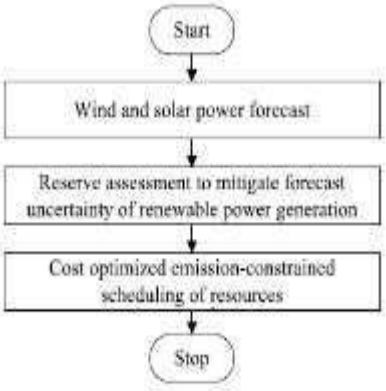

International Journal Of Core Engineering & Management (ISSN: 2348-9510)
Special Issue, NCIAEE-2017, St. Johns College of Engineering and Technology, Yemmiganur

Fig 4: Overview of optimized scheduling approach

Optimal control Problems (OCPs)

OCPs make explicit use of the system model, given by in order to find an optimal control law u* (.), which meets number of equality and inequality constraints. The term optimal here is defined with respect to a certain criterion that implies the control objectives. This criterion is specified with a cost functional J, consisting of the Lagrangian term $\mathcal{L}$ and the terminal cost term $\mathcal{M}$. While the Lagrangian term indicates the cost function during the period of time T, the terminal cost penalizes final values. Equations (11d) and (11e), respectively, formulate the final and initial constraints which must be maintained by the optimal solution.

The developed NMPC controller consists of three entities:

1) the dynamic optimizer that successively solves OCP at each sampling time *h*, defined in Table I; 2) the mathematical model, $\mathcal{F}$, of the system to predict its behavior; and 3) the cost function and constraints of the relevant OCP. The optimal pitch angle, β, is applied as a set point to an inner closed-loop controller. More-over, the optimal values of the switching duty cycles are applied to the pulse width modulators (PWMs) of the dc-dc converters.

TABLE I

WIND TURBINE, PMSG, BATTERY STACK, AND PV PARAMETERS IN THIS STUDY

Wind turbine		PMSG		Battery stack		PV array	
$C_1(-)$	0.517	$J(Kg.m^2)$	0.35	$C_{max}(Ah)$	48.15	$R_s(\Omega)$	0.221
$C_2(-)$	116.0	$F(N.m.s)$	0.002	$R_{bat}(\Omega)$	0.019	$R_{sh}(\Omega)$	405.4
$C_3(-)$	0.4	$P(-)$	8	$V_0(V)$	12.3024	$n_d(-)$	1.3
$C_4(-)$	5.0	$\psi(V.s)$	0.8	$P_1(-)$	0.9	$N_s(-)$	54
$C_5(-)$	21.0	$P_{rated}(KW)$	10.0	$N_{bats}(-)$	8	$I_{sc,stc}(A)$	8.21
$C_6(-)$	0.007	$L_s(H)$	0.0083	$N_{batp}(-)$	3	$V_{oc,stc}(V)$	32.9
$\lambda_{opt}(-)$	8.1			$T_s(sec)$	0.726	$k_I(A/K)$	0.003
$P_{wt,nom}(KW)$	10.0			$V_{bstack,nom}(V)$	96.0	$k_V(V/K)$	-0.12
Rad (m)	4.01			$P_{bat,nom}(KW)$	1.296	$N_{pvs}(-)$	1
$U_{x,base}(m/s)$	12.0			$C_{10}(Ah)$	45.0	$N_{pvp}(-)$	10
$C_{p,max}(-)$	0.48			$V_{gas}(V)$	13.0	$P_{pv,nom}(KW)$	2.001

Predictive control

(MPC) is an advanced method of process control that has been in use in the process industries in chemical plants and oil refineries since the 1980s. In recent years it has also been used in power system balancing models.[1] Model predictive controllers rely on dynamic models of the process, most often linear empirical models obtained by system identification. The main advantage of MPC is the fact that it allows the current timeslot to be optimized, while keeping future timeslots in account. This

is achieved by optimizing a finite time-horizon, but only implementing the current timeslot. MPC has the ability to anticipate future events and can take control actions accordingly.PID and LQR controllers do not have this predictive ability. MPC is nearly universally implemented as a digital control, although there is research into achieving faster response times with specially designed analog circuitry.

IV. RESULTS AND DISCUSSION

Table shows the parameters of different components and their values in this study. The linear load demand is also less than or equal to 12 KW. Two test scenarios are carried out to evaluate the performance of the developed optimal EMS.

Scenario I: Constant Current Charging Mode

Fig. 5(a) illustrates the normalized wind speed, insolation, and load demand inputs to the system. Wind speed starts at the rating value of the generator and sharply increases by 37.5% at t = 600 s. Load demand is below the nominal value, except between 300 to 600 s. Moreover, solar irradiance is constant during the simulation only for results clarification.

Fig. 5(b)–(e) depicts the calculated optimal control variables. Applying these optimal control variables to standalone dc microgrid, different variables of the wind and solar branches are depicted in Fig. 6. Fig. 7 illustrates the resulting dc bus voltage and the battery bank SOC and charging currents.

The wind branch operates at MPPT mode up to t = 300 seconds with a calculated pitch angle of zero as given in fig 5(b). Fig 5(c) shows the calculated buck converter duty cycle that adjusts the rotational speed of the wind turbine at its nominal value, as given by Fig 6(a). Fig 6(b) indicates that the resulting power coefficient reaches to its maximum value.

At t = 300 and 600 s, the pitch angle goes up to 1.2 and 16 degrees, respectively, to promote pitching to feather [23]. Fig. 6(a) and (b) illustrates a combination of the speed and power coefficient variations that curtails the generation down to 9.039 KW after t = 600 s, as given by Fig. 6(e).

Fig. 6(c) and (d) illustrates that though the PV array initially operates at its MPP, i.e., V_{pv} = 26.3 V and I_{pv} = 76.1 A, the controller curtails its generation down to 1.808 KW [Fig 6(f)] after t = 600s. Therefore, the power sharing deficiency is 0.035% which is within the permissible range of $\pm$1%. It should be noted that $\alpha_2 \neq 0$ causes a slight inaccuracy in the wind power generation which can be reduced by decreasing the design parameter α_2.

In spite of significant wind speed and load demand variations, Fig. 7(a) depicts that the dc bus voltage level stays within the permissible range, i.e., 48.0 $\pm$ 0.96 V. From Fig 7(a), it can be seen that after t = 300s, when there is not enough generated power to charge battery, controller reduces the dc bus voltage level. However, at t = 600s the voltage level returns back to the nominal value.

Fig 7(b) depicts that the charging current of the battery bank remains constant at its nominal value, i.e., $0.15C_{10}$, before t = 300 and after t = 600s. Although at t = 600s the charging current initially exceeds the nominal value, it returns back because of generation curtailment. In Fig 7(c), it can be seen that this strategy helps the battery to be charged up to high State of Charge values of battery.

International Journal Of Core Engineering & Management (ISSN: 2348-9510)
Special Issue, NCIAEE-2017, St. Johns College of Engineering and Technology, Yemmiganur

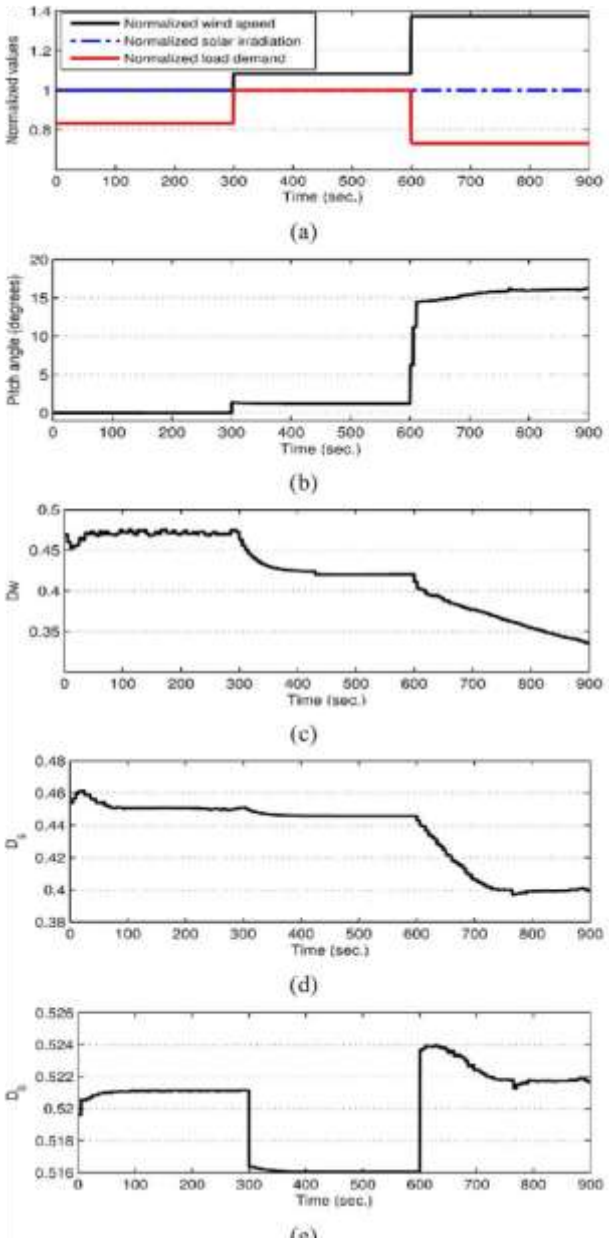

Fig 5 (a) Normalized amounts of non-manipulated inputs and the optimal (b) pitch angle, and switching duty cycles of the (c) wind, (d) solar and (e) battery branch converters in Scenario I.

B. Scenario II: Constant Voltage Charging Mode

Once the battery terminal voltage reaches the gassing voltage, the charging current should be gradually reduced in order to maintain the voltage below the gassing level and fully charge the

International Journal Of Core Engineering & Management (ISSN: 2348-9510)
Special Issue, NCIAEE-2017, St. Johns College of Engineering and Technology, Yemmiganur

battery without the risk of permanent damage. For this purpose, the cost function of the developed NMPC strategy is switched.

For the same wind speed and isolation variations as Scenario I, Fig 8(a) and (b), respectively, shows the charging current and terminal voltage variations of the battery bank. From Fig 8(a), it can be seen that the battery bank is charged with a constant current equals to $0.31C_{10}$ up to t = 300s when the terminal voltage reaches to 99.2%, as a safe margin, of the gassing voltage. Then, the controller starts gradually reducing the charging

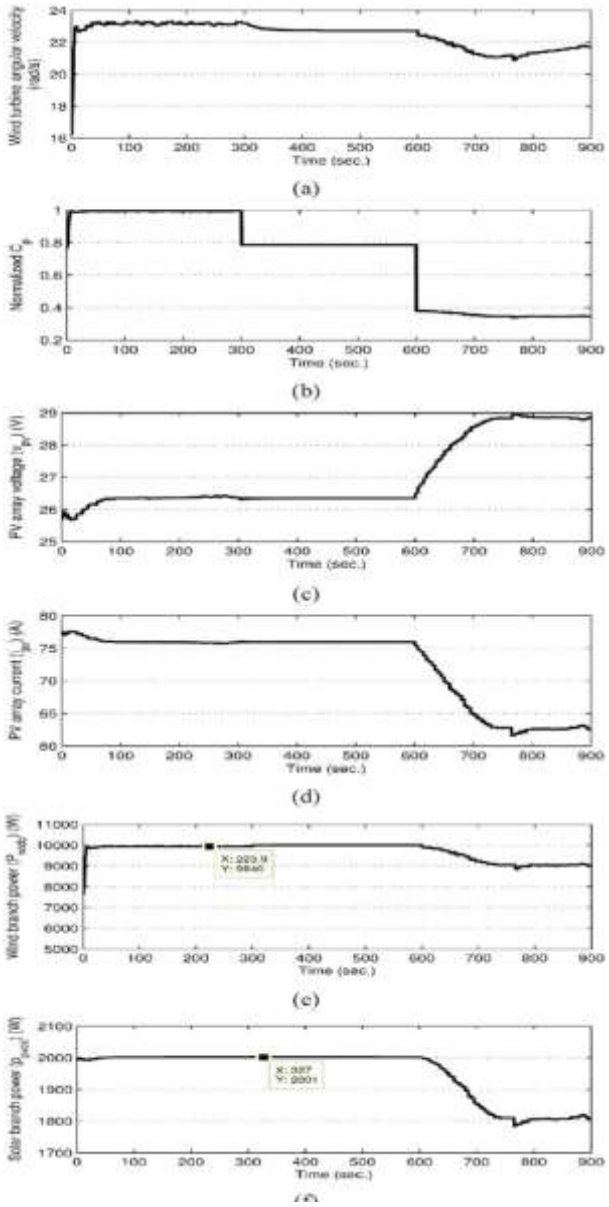

International Journal Of Core Engineering & Management (ISSN: 2348-9510)
Special Issue, NCIAEE-2017, St. Johns College of Engineering and Technology, Yemmiganur

Fig 6 Different variables of the wind and solar branches: the wind turbine (a) angular velocity and (b) power coefficient; the PV array (c) voltage and (d) current; and (e)-(f) the generated power by each branch in Scenario I.

current in order to maintain the battery bank voltage constant. Fig 8(c) indicates that the battery can be fully charged with the constant current-constant voltage regime with no risk of exceeding the gassing voltage.

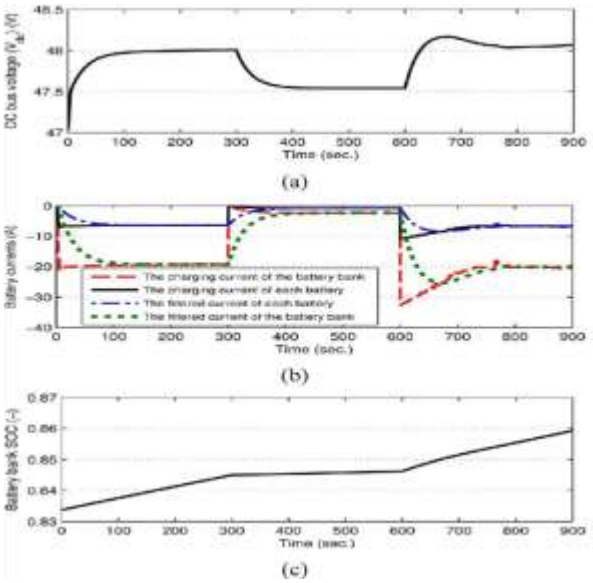

Fig 7 (a) The dc bus voltage of the microgrid, (b)charging current, and (c) SOC of the battery bank in Scenario I.

International Journal Of Core Engineering & Management (ISSN: 2348-9510)
Special Issue, NCIAEE-2017, St. Johns College of Engineering and Technology, Yemmiganur

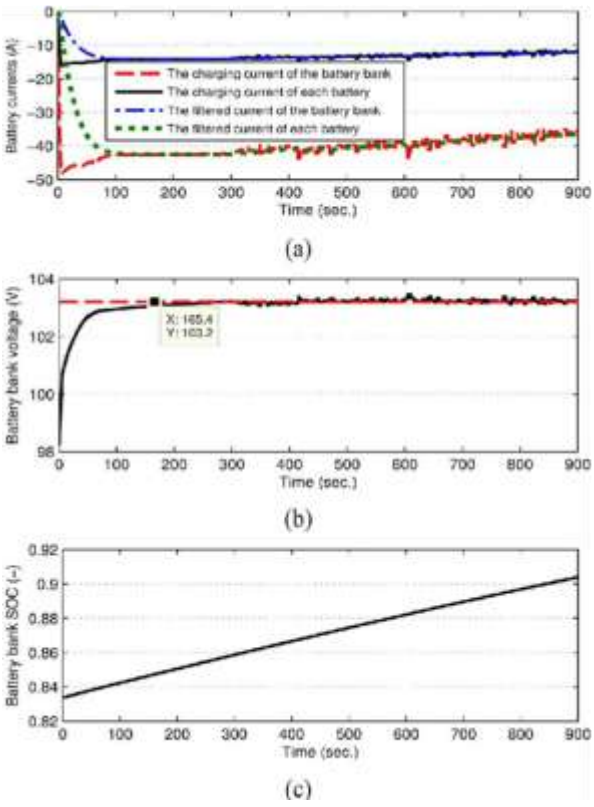

Fig 8 (a) Charging current, (b) terminal voltage and (c)SOC of the battery bank in Scenario II.

V. CONCLUSION AND FUTURE WORKS

In this paper, we developed a novel optimal EMS that manages the energy flows across a standalone green dc microgrid, consisting of the wind, solar, and battery branches. A coordinated and multivariable online NMPC strategy has been developed to address, as the optimal EMS, three main control objectives of standalone dc microgrids. These objectives are the voltage level regulation, proportional power sharing, and battery management. In order to address these objectives, the developed EMS simultaneously controls the pitch angle of the wind turbine and the switching duty cycles of three dc-dc converters. It has been shown that the developed controller tracks the MPPs of the wind and solar branches within the normal conditions and curtails their generations during the underload conditions. The provided flexible generation curtailment strategy realizes the constant current-constant voltage charging regime that potentially increases the life span of the battery bank. It is important to note that the proposed strategy can be employed as a centralized implementation of the primary and secondary levels in the hierarchical architecture. The simulation results have shown its ability to achieve all control objectives. The issue of considering the discharging mode of the battery operation, which shifts the problem to the class of hybrid dynamical systems, is currently being investigated.

REFERENCES

[1] J. M. Guerrero, M. Chandorkar, T. Lee, and P. C. Loh, "Advanced Control Architectures for Intelligent Microgrids-Part I: Decentralized and Hierarchical Control," *IEEE Trans. Ind. Electron.*, vol. 60, no. 4, pp. 1254–1262, 2013.
[2] R. S. Balog, W. W. Weaver, and P. T. Krein, "The load as an energy asset in a distributed DC smartgrid architecture," *IEEE Trans. Smart Grid*, vol. 3, no. 1, pp. 253–260, 2012.
[3] J. M. Guerrero, P. C. Loh, T. L. Lee, and M. Chandorkar, "Advanced Control Architectures for Intelligent Microgrids-Part II: Power quality, energy storage, and AC/DC microgrids," *IEEE Trans. Ind. Electron.*, vol. 60, no. 4, pp. 1263–1270, 2013.
[4] N. Eghtedarpour and E. Farjah, "Control strategy for distributed inte-gration of photovoltaic and energy storage systems in DC micro-grids," *Renew. Energy*, vol. 45, no. 0, pp. 96–110, 2012.
[5] D. Chen and L. Xu, "Autonomous DC voltage control of a DC micro-grid with multiple slack terminals," *IEEE Trans. Power Syst.*, vol. 27, no. 4, pp. 1897–1905, Nov. 2012.
[6] L. Xu and D. Chen, "Control and operation of a DC microgrid with variable generation and energy storage," *IEEE Trans. Power Del.*, vol. 26, no. 4, pp. 2513–2522, Oct. 2011.
[7] S. Anand, B. G. Fernandes, and M. Guerrero, "Distributed control to ensure proportional load sharing and improve voltage regulation in low-voltage DC microgrids," *IEEE Trans. Power Electro.*, vol. 28, no. 4, pp. 1900–1913, 2013.
[8] B. Zhao, X. Zhang, J. Chen, C. Wang, and L. Guo, "Operation opti-mization of standalone microgrids considering lifetime characteristics of battery energy storage system," *IEEE Trans. Sustain. Energy*, to be published.
[9] T. Zhou and B. Francois, "Energy management and power control of a hybrid active wind generator for distributed power generation and grid integration," *IEEE Trans. Ind. Electron.*, vol. 58, no. 1, pp. 95–104, 2011.
[10] X. Liu, P. Wang, and P. C. Loh, "A hybrid AC/DC microgrid and its co-ordination control," *IEEE Trans. Smart Grid*, vol. 2, no. 2, pp. 278–286, 2011.
[11] H. Kanchev, D. Lu, F. Colas, V. Lazarov, and B. Francois, "Energy management and operational planning of a microgrid with a PV-based active gen. for smart grid applications," *IEEE Trans. Ind. Electron.*, vol. 58, no. 10, pp. 4583–4592, 2011.
[12] H. Ghoddami, M. B. Delghavi, and A. Yazdani, "An integrated wind-photovoltaic-battery system with reduced power-electronic interface and fast control for grid-tied and off-grid applications," *Renew. Energy*, vol. 45, no. 0, pp. 128–137, 2012.
[13] J. M. Guerrero, J. C. Vasquez, J. Matas, L. G. de Vicua, and M. Castilla, "Hierarchical control of droop-controlled AC and DC microgrids-a general approach toward standardization," *IEEE Trans. Ind. Electron.*, vol. 58, no. 1, pp. 158–172, 2011.
[14] P. H. Divshali, A. Alimardani, S. H. Hosseinian, and M. Abedi, "De-centralized cooperative control strategy of microsources for stabilizing autonomous VSC-Based microgrids," *IEEE Trans. Power Syst.*, vol. 27, no. 4, pp. 1949–1959, Nov. 2012.
[15] P. C. Loh, D. Li, Y. K. Chai, and F. Blaabjerg, "Autonomous operation of hybrid microgrid with AC and DC subgrids," *IEEE Trans. Power Electron.*, vol. 28, no. 5, pp. 2214–2223, 2013.
[16] T. L. Vandoorn, B. Meersman, L. Degroote, B. Renders, and L. Van-develde, "A control strategy for islanded microgrids with DC-Link voltage control," *IEEE Trans. Power Del.*, vol. 26, no. 2, pp. 703–713, Apr. 2011.
[17] T. L. Vandoorn, B. Meersman, J. D. M. De Kooning, and L. Vande-velde, "Analogy between conventional grid control and islanded mi-crogrid control based on a global DC-Link voltage droop," *IEEE Trans. Power Del.*, vol. 27, no. 3, pp. 1405–1414, Jul. 2012.

[18] H. Kakigano, Y. Miura, and T. Ise, "Distribution voltage control for DC microgrids using fuzzy control and gain-scheduling technique," *IEEE Trans. Power Electron.*, vol. 28, no. 5, pp. 2246–2258, 2013.
[19] H. Fakham, D. Lu, and B. Francois, "Power control design of a battery charger in a hybrid active PV generator for load-following applications," *IEEE Trans. Ind. Electron.*, vol. 58, no. 1, pp. 85–94, 2011.
[20] A. M. Dizqah, A. Maheri, K. Busawon, and P. Fritzson, "Acausal mod-elling and dynamic simulation of the standalone wind-solar plant using modelica," in *Proc. 2013 15th Int. Conf. Computer Modelling and Sim-ulation (UK-Sim)*, 2013, pp. 580–585.
[21] A. Meharrar, M. Tioursi, M. Hatti, and A. B. Stambouli, "A variable speed wind generator maximum power tracking based on adaptative neuro-fuzzy inference system," *Expert Syst. Applicat.*, vol. 38, no. 6,7659–7664, 2011.
[22] H. Li and Z. Chen, "Overview of different wind generator systems and their comparisons," *IET Renew. Power Gener.*, vol. 2, no. 2, pp. 123–138, 2008.
[23] T. Burton, N. Jenkins, D. Sharpe, and E. Bossanyi, *Wind Energy Hand-book*, 2nd ed. New York, NY, USA: Wiley, 2011.
[24] S. Heier, *Grid Integration of Wind Energy Conversion Systems*. New York, NY, USA: Wiley, 1998.
[25] N. Mohan, T. M. Undeland, and W. P. Robbins, *Power Electronics: Converters, Applications, and Design*. New York, NY, USA: Wiley, 1995.
[26] O. Tremblay and L. Dessaint, "Experimental validation of a battery dynamic model for EV applications," *World Elect. Vehicle J.*, vol. 3,10–15, 2009.
[27] J. J. Soon and K. S. Low, "Photovoltaic model identification using par-ticle swarm optimization with inverse barrier constraint," *IEEE Trans. Power Electron.*, vol. 27, no. 9, pp. 3975–3983, 2012.
[28] M. G. Villalva, J. R. Gazoli, and E. R. Filho, "Comprehensive ap-proach to modeling and simulation of photovoltaic arrays," *IEEE Trans. Power Electron.*, vol. 24, no. 5, pp. 1198–1208, 2009.
[29] A. M. Dizqah, K. Busawon, and P. Fritzson, "Acausal modeling and simulation of the standalone solar power systems as hybrid DAEs," in
Proc. 53rd Int. Conf. Scandinavian Simul. Soc., 2012.

[30] R. Findeisen and F. Allgwer, "An introduction to nonlinear model pre-dictive," in *Proc. 21st Benelux Meeting Syst. and Control*, Veidhoven, The Netherlands, 2002, pp. 1–23.